

Topological Pumping in Doubly Modulated Mechanical Systems

Yunhong Liao^{ID} and Xiaoming Zhou^{ID*}

Key Laboratory of Dynamics and Control of Flight Vehicle, Ministry of Education and School of Aerospace Engineering, Beijing Institute of Technology, Beijing 100081, China



(Received 14 January 2022; revised 1 March 2022; accepted 4 March 2022; published 31 March 2022)

Topological pumping allows higher-dimensional topological phenomena to be explored in low-dimensional systems using synthetic dimension with time modulation. Extensive studies have been devoted to the one-dimensional pumping lattice with singly modulated parameters, which was shown to exhibit the mechanical-wave analog of the quantum Hall effect. Here, we study the topological pumping in the lattice chain with doubly modulated parameters, and report the theoretical finding of two additional topological phases with the large-gap Chern number, which has not been well disclosed previously in singly modulated mechanical systems. The edge state protected by the large-gap Chern number exhibits the faster edge-to-edge energy transportation under the slow temporal variation of modulating parameters. The adiabatic approximation of doubly modulated pumping is also analyzed, and it would not be violated in the process of the fast-pumping evolution of edge states. The finding is expected to be used for fast and robust energy transportation of mechanical waves.

DOI: 10.1103/PhysRevApplied.17.034076

I. INTRODUCTION

Topological phase of matters has attracted extensive attention over recent years across different realms of physics [1,2]. One of the most remarkable properties of topological phase is the band-gap-crossing edge state that exhibits unidirectional transport, and due to the intrinsic topological protection of bulk bands, the edge state exists stably as long as the band gap remains open, showing strong robustness against a wide range of defects and disorders. Although initially discovered in electronic systems, the exploration for topological states was rapidly extended to classical wave systems [3,4]. Analogs of topological insulators have been subsequently reported and realized in the form of the photonic [5–7], phononic crystals [8,9], and metamaterials [10,11] with robust wave-propagation phenomena that revolutionize our understanding.

Topological phases could also be constructed in synthetic spaces. Based on the adiabatic theorem, broad interests have been stimulated in exploiting synthetic dimensions for achieving higher-dimensional topological states in low-dimensional physical systems [12–17]. In the early stage, quantized charge transport was predicted in a one-dimensional (1D) electronic system under a slow cyclic variation of a periodic potential, which was later known as the Thouless pump [18]. The charge pumped per cycle was associated with the Chern number defined on the synthetic two-dimensional (2D) Brillouin zone spanned by momentum and time. Meanwhile the 2D Hofstadter

model [19], an electronic square lattice in the presence of a perpendicular magnetic field, was equivalently mapped onto the 1D Aubry-Andre model that features the periodically modulated parameter [20]. These findings reveal that the 1D adiabatic pumping process can be regarded as the dynamical manifestation of the 2D Chern insulator, so it is also protected by the intrinsic topology.

The topological pumping effect was later extended to classical wave systems, and exploited in optical lattices [21–23], photonic waveguide arrays [24–26], acoustic waveguides [27–36], as well as elastic plates or beams [37–42]. The topologically protected energy manipulation is pursued through the dynamic evolution in additional spatial or temporal dimensions. For instance, dynamically controlled optical superlattices are used to modulate the on-site potential of ultracold bosonic atoms [21]. Periodically arranged photonic waveguides are utilized to realize the adiabatic evaluation of the hopping strength (or the on-site potential) by engineering the interwaveguide spacing (or the refractive index) [25,26]. Acoustic waveguides characterized by the moving mechanical boundary condition are demonstrated to possess the robust energy pumping [27,28]. In mechanical systems, the stiffness of elastic waveguides or plates is modulated in two spatial dimensions to construct the topological pumping states spanning nontrivial gaps [40,42]. Alternatively, the topological pump can be constructed in beams with the temporal modulation of stiffness as an additional synthetic dimension, which are devised by the magnetically coupled mechanical resonators or shunted piezoelectric patches [37,41]. By involving the temporal modulation of parameters, the

*zhxming@bit.edu.cn

temporal topological pump provides a unique platform to explore higher-order topological states in low-dimensional systems.

In pumping systems with more modulating parameters, topological phases with larger Chern numbers can be created and used for faster energy transportation. These have been demonstrated in quantum and optical systems [26,43]. However, the issue is rarely explored in mechanical systems. The present study focuses on the 1D topological pumping, and by temporally modulating two sets of parameters, richer topological phases than those found in singly modulated systems would be disclosed. The doubly modulated parameters are engineered by dynamic mechanism structures, which are physically realizable and also provide a clear illustration of energy exchange with surroundings during the adiabatic evolution of eigenstates. Lastly, the adiabatic approximation condition is analyzed for the topological pumping in doubly modulated mechanical systems.

II. THEORETICAL FORMULATION

Consider a 1D lattice chain consisting of identical mass blocks of weight m linked by linear springs k_c , and each mass is constrained by ground springs k_g as shown in Fig. 1. The 1D lattice, if modulated only in space, is characterized by a band topology in the wave-vector domain. To create the 2D topological effect in the 1D lattice, one can introduce a slow temporal variation of model parameter that acts as the synthetic dimension according to the concept of Thouless pump [18]. This has been studied in 1D mass-spring lattice featuring the modulated interconnected spring [44,45] or in the quasiperiodic continuous elastic beams with the modulated ground springs [46]. In

contrast to previous studies, we consider here the temporal modulation of both springs k_c and k_g , and explore the topological nontrivial phases in 2D parameter space spanned by the wave vector and time-modulated phase.

In our model, the temporal modulation of $k_c(t)$ and $k_g(t)$ is implemented by using rotary-mechanism structures, which has been proven efficient for time modulation of mechanical properties [47,48]. The dynamic modulation mechanism introduced here is characterized by elastic springs that rotate along an axis vertical to the lattice direction as illustrated in Fig. 1. For temporal modulation of $k_g(t)$, a pair of springs of tension stiffness k_1 rotate with the angular frequency ω_r from an initial biasing angle ϕ_g . This would produce the time-periodic elastic constraint to the mass block [48] as given by

$$k_g(t) = k_1 + k_1 \cos(\phi + 2\phi_g), \quad (1)$$

where $\phi = \omega_m t = 2\omega_r t$, and ω_m refers to the modulating frequency. Adjacent mass bodies are connected by a constant spring k_0 and another pair of springs k_2 that rotate with identical angular frequency ω_r from initial angle ϕ_c . Through the homogenization analysis, the rotary-spring mechanism attached in between adjacent mass bodies realizes the modulated stiffness $k_c(t)$, given by

$$k_c(t) = k_0 + k_2 + k_2 \cos(\phi + 2\phi_c). \quad (2)$$

Consider the case that the supercell of the infinite lattice contains three elements. The spatiotemporal modulation of stiffness can be achieved when different initial angles of rotary mechanisms are assigned for each element. The general expressions of modulated stiffnesses for the i th

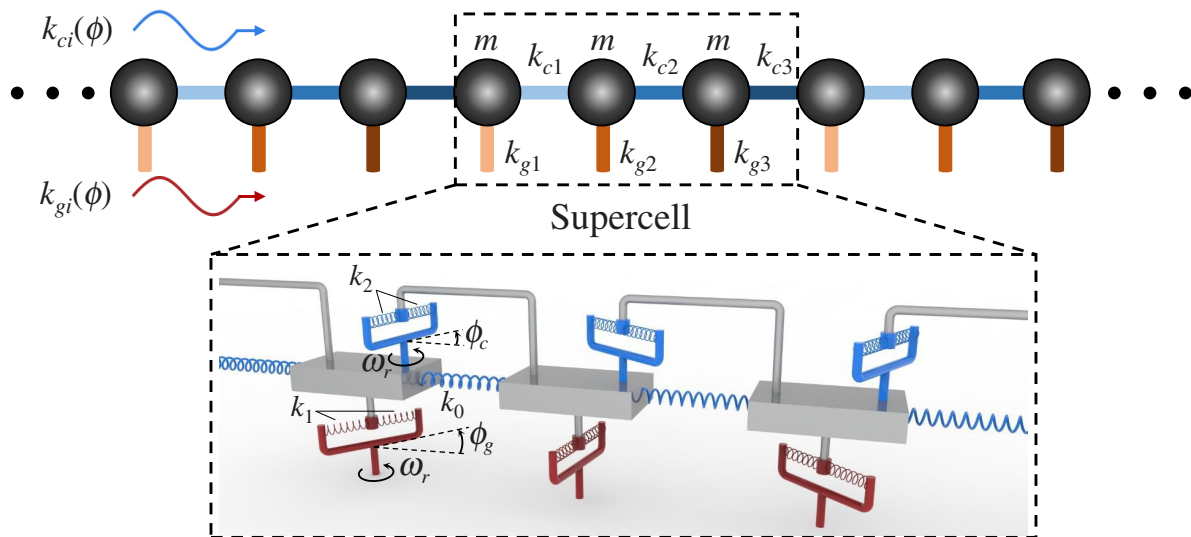


FIG. 1. 1D topological pumping model consisting of the mass-spring lattice chain where the ground spring and interelement spring are temporally modulated simultaneously.

element ($i = 1, 2, 3$) in each supercell can be written as

$$k_{gi}(\phi) = k_1 + k_1 \cos[\phi + 2(i-1)\pi/3 + \delta\phi_0], \quad (3)$$

$$k_{ci}(\phi) = k_0 + k_2 + k_2 \cos[\phi + 2(i-1)\pi/3], \quad (4)$$

where $\delta\phi_0 = 2\phi_g - 2\phi_c$ denotes the initial phase contrast. Consider the slow variation of modulated stiffness over time such that the system could be regarded as being quasistatic (or adiabatic) at each moment characterized by phase ϕ . By imposing the Bloch periodic condition to the supercell, the instantaneous eigenvalue equation can be written in terms of the displacement \mathbf{u} as

$$\mathbf{K}(q, \phi)\mathbf{u} = \omega^2 \mathbf{M}\mathbf{u}, \quad (5)$$

where q denotes the Bloch phase, ω is the eigenfrequency, and $\mathbf{M} = m\mathbf{I}_3$ with \mathbf{I}_3 referring to the identity matrix of size 3. $\mathbf{K}(q, \phi) = \mathbf{K}_g(\phi) + \mathbf{K}_c(q, \phi)$ is the stiffness matrix, where $\mathbf{K}_g(\phi)$ and $\mathbf{K}_c(q, \phi)$ are relevant to the modulated ground spring and interelement spring, respectively, and are given by

$$\mathbf{K}_g(\phi) = \begin{bmatrix} k_{g1} & 0 & 0 \\ 0 & k_{g2} & 0 \\ 0 & 0 & k_{g3} \end{bmatrix} \quad (6)$$

$$\mathbf{K}_c(q, \phi) = \begin{bmatrix} k_{c3} + k_{c1} & -k_{c1} & -k_{c3}e^{-iq} \\ -k_{c1} & k_{c2} + k_{c1} & -k_{c2} \\ -k_{c3}e^{iq} & -k_{c2} & k_{c2} + k_{c3} \end{bmatrix} \quad (7)$$

By solving Eq. (5), one can calculate the eigenstate $\mathbf{u}(q, \phi)$ of the 1D lattice for specific ϕ . When the slow temporal variation of ϕ is performed, it would lead to a phase accumulation, which is responsible for nontrivial topology in the synthetic 2D system spanned by (q, ϕ) . The topological property is characterized by the Chern number defined

on $(q, \phi) \in D = [-\pi, \pi] \times [0, 2\pi]$ in the form of [49]

$$C = \frac{1}{2\pi i} \iint_D \nabla \times \mathbf{A} dD, \quad (8)$$

where $\nabla = (\partial/\partial q)\mathbf{e}_q + (\partial/\partial \phi)\mathbf{e}_\phi$ and $\mathbf{A} = \mathbf{u}^* \cdot \nabla \mathbf{u}$ with $(\cdot)^*$ denoting a complex conjugate operation. In what follows, the eigenstate evolution against ϕ is analyzed to explore nontrivial topological phases for different sets of parameters k_1 , k_2 , and $\delta\phi_0$.

III. RESULTS AND DISCUSSIONS

A. Topological phases in doubly modulated systems

Consider parameters $m = 0.1$ kg and $k_0 = 2$ kN/m. Figure 2(a) plots the dispersion surface in the (q, ϕ) space as calculated from Eq. (5) for a set of parameters $k_1 = k_2 = k_0$, $\delta\phi_0 = 2\pi/3$. The result shows three bulk bands separated by gaps, and we denote the Chern number of bulk bands by C_i ($i = 1, 2, 3$). The Chern numbers (C_1, C_2, C_3) realized here are $(-1, 2, -1)$, termed as type-I topological phase, which has already been observed in a singly modulated system [44,45]. When the parameter is changed to $k_1 = 3k_0$, three separate dispersion bands still exist but with different Chern numbers $(-1, -1, 2)$, as shown in Fig. 2(b), which we call the type-II topological phase. When another set of parameters $k_1 = k_2 = 2k_0$, $\delta\phi_0 = 5\pi/3$ is chosen, a third type of topological phase with Chern numbers $(2, -1, -1)$ (type-III) can be found. The latter two phases, not well disclosed in mechanical systems previously, manifest themselves by the permutation of Chern numbers $-1, 2$, and -1 . This implies the existence of phase transition between them, which needs to be made clear in order to identify the correlation of different topological phases. On the other hand, despite the fact that they differ only by permutation, the gap Chern number, which equals the summation of Chern numbers of all bulk bands below the gap, would be drastically different. According to the principle of bulk-edge correspondence,

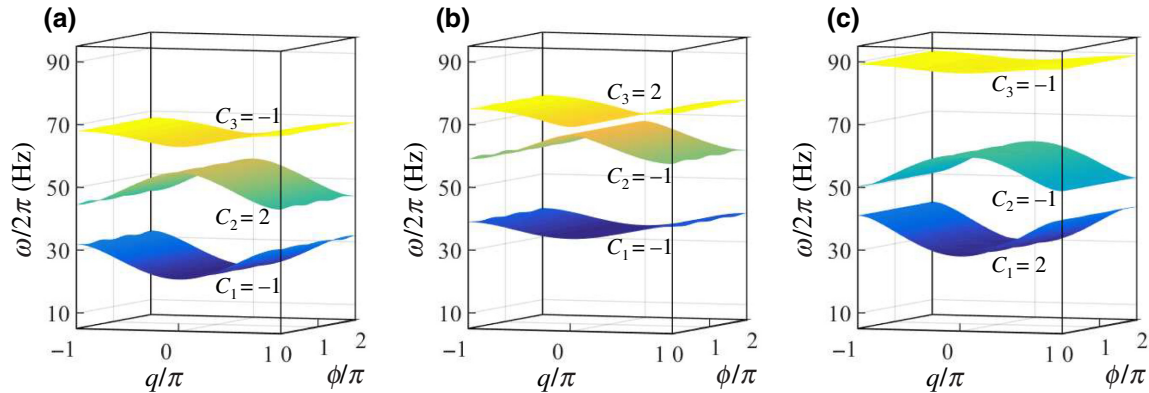


FIG. 2. Dispersion surfaces in the (q, ϕ) space for different sets of parameters: (a) $k_1 = k_2 = k_0$, $\delta\phi_0 = 2\pi/3$; (b) $k_1 = 3k_0$, $k_2 = k_0$, $\delta\phi_0 = 2\pi/3$; and (c) $k_1 = k_2 = 2k_0$, $\delta\phi_0 = 5\pi/3$.

richer pumping responses of edge states can be expected, as addressed below.

To clarify the transition among different phases, we classify topological phases in the parameter space $(\kappa_1, \kappa_2, \delta\phi_0)$, as shown in Fig. 3(a), where normalized parameters $\kappa_1 = k_1/k_0$ and $\kappa_2 = k_2/k_0$ are used. It is found that the type-II and type-III phase zones share no boundaries, and they have the cone shapes with the vertex points at $(0, 0, 2\pi/3)$ and $(0, 0, 5\pi/3)$, respectively. By choosing the specific value of $\delta\phi_0 = 2\pi/3$, the 2D phase distribution is plotted in Fig. 3(b), showing that the type-II phase region can be enlarged as the values of κ_1 and κ_2 increase. Besides, there exists the characteristic line of the tangent $\kappa_1/\kappa_2 = 3$, and for every point on the line except zero the type-II phase is preserved without transition to type-I phase. Since topological phase transitions relate to the band-gap closure, we plot the frequency range of band gaps for various κ_2 by choosing $\kappa_1 = 3$ as shown by the shaded region in Fig. 3(d). The phase transition points at $\kappa_2 \approx 0.7$ and $\kappa_2 \approx 1.2$ are found to correlate the closing and reopening of the second band gap, while the first band gap remains open. This accounts for the fact that the Chern numbers C_2 and C_3 for type-II $(-1, -1, 2)$ and type-I $(-1, 2, -1)$ phases are exchanged, while the Chern number $C_1 = -1$ remains unaltered. The characteristics of type-III phase $(2, -1, -1)$ can be understood in the similar manner. Figure 3(c) shows the 2D phase distribution for $\delta\phi_0 = 5\pi/3$, where the characteristic line with the tangent $\kappa_1/\kappa_2 = 1$ can be found for the type-III phase. In the case of $\kappa_1 = 1$, the transition points at $\kappa_2 \approx 0.5$ and $\kappa_2 \approx 2.7$ correspond to the closing of the first band gap, which results in the interchange of Chern numbers C_1 and C_2 . In this case, the second band gap is always opening, thus C_3 is unchanged upon the transition between type-I and type-III phases.

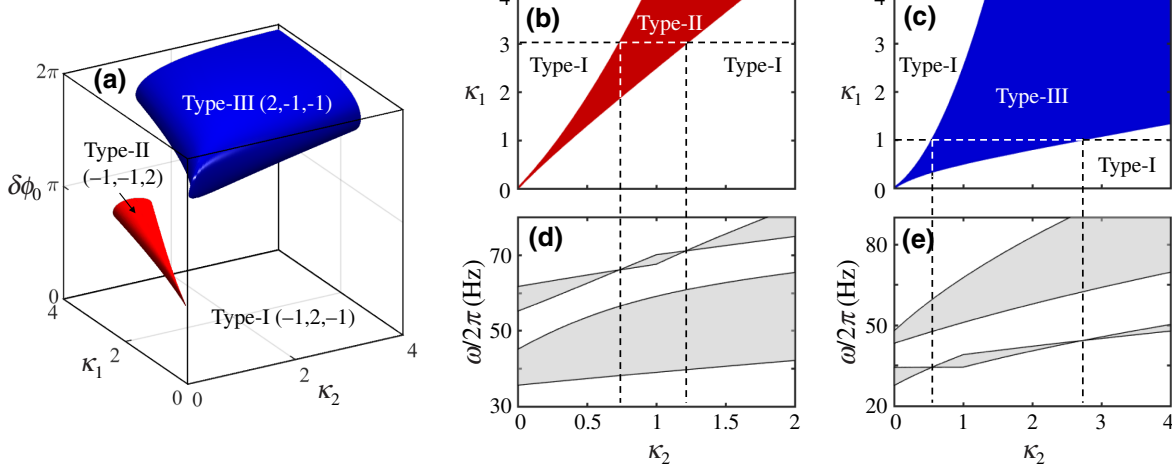


FIG. 3. Topological phase transition and associated band-gap variation. (a) Classification of topological phases in the parameter space $(\kappa_1, \kappa_2, \delta\phi_0)$; (b) the 2D phase distribution for specific values of $\delta\phi_0 = 2\pi/3$ and (d) the frequency range of band gaps (shaded region) for various κ_2 when $\kappa_1 = 3$ is chosen; (c),(e) results corresponding to (b),(d), but with $\delta\phi_0 = 5\pi/3$ and $\kappa_1 = 1$.

B. Analysis of topological pumping responses

Three types of topological phases are shown to possess the nonzero Chern numbers, which imply the existence of topological edge states according to the principle of bulk-edge correspondence [50,51]. The topological behavior of edge states is decided by the gap Chern number C_g , which is the summation of Chern numbers below the gap. For the type-I topological phase $(-1, 2, -1)$ as shown in Fig. 2(a), the gap Chern number is $C_g = C_1 = -1$ for the lower band gap, while $C_g = C_1 + C_2 = 1$ for the higher one. The fact that C_g equals one for both gaps predicts that there exists one pumping cycle of edge-state evolution, and the opposite sign indicates the different evolution direction [44,45]. To confirm the existence of topological edge states, the eigenstates of the modulated lattice with 20 supercells and free boundary conditions on both sides are solved, where the parameters of the supercell are the same as those considered in Fig. 2(a). Figure 4(a) shows the eigenfrequency against the variation of evolution phase ϕ . The edge states between bulk modes, which are localized on either left or right boundaries, can be clearly distinguished. To demonstrate the pumping behavior of edge states, we perform the time-domain response computation of the finite lattice subject to the narrow-band impulse excitation with the applied force

$$F = A_0 e^{-[(t-n_c T_c)\omega_c/n_0]^2} \cos(\omega_c t), \quad (9)$$

where A_0 is the amplitude, ω_c is the central frequency with the time period of $T_c = 2\pi/\omega_c$, n_c and n_0 determine the arrival time of pulses and the frequency bandwidth, respectively. To guarantee the adiabatic evolution of eigenstates, we consider a very slow temporal modulation with the frequency $\omega_m = 2\pi \times 10^{-3}$ rad/s. More detailed analysis of adiabatic evolution condition will be conducted in the

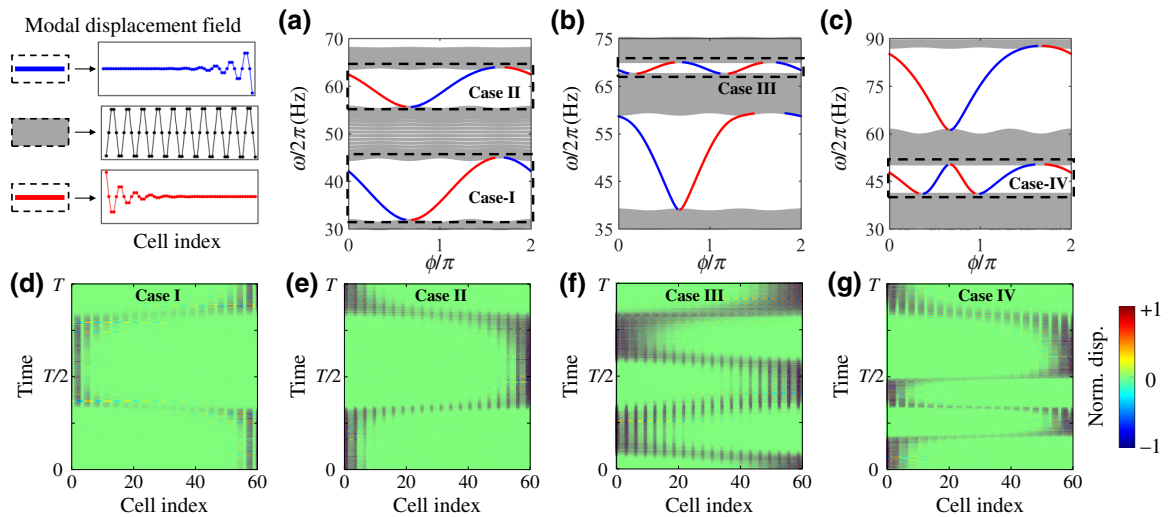


FIG. 4. Eigenstates of finite lattices and their impulse responses. (a)–(c) Eigenfrequency of the finite lattice chain comprising 20 supercells against the variation of ϕ , corresponding to three cases in Figs. 2(a)–2(c); the time-domain impulse responses of the finite lattice in four cases: (d) $\omega_c/2\pi = 42.1$ Hz, $n_0 = 400$, $n_c = 200$, (e) $\omega_c/2\pi = 62.4$ Hz, $n_0 = 400$, $n_c = 200$, (f) $\omega_c/2\pi = 68.4$ Hz, $n_0 = 600$, $n_c = 300$, and (g) $\omega_c/2\pi = 47.7$ Hz, $n_0 = 400$, $n_c = 200$ with the same pulse amplitude $A_0 = 0.1$.

next section. By properly choosing the central frequency of impulse excitation, the adiabatic evolution propagation of edge states at lower and higher frequency bands can be excited, as illustrated by the time-domain displacement responses of the finite lattice in Figs. 4(d) and 4(e), respectively. In the time period ($0 \leq t \leq T = 2\pi/\omega_m$) that the phase ϕ varies from 0 to 2π , the edge state initially localized at either left or right side is firstly transferred to the opposite edge, and then returning back, realizing one complete cycle of topological pumping. These behaviors are consistent with the prediction by the gap Chern number $|C_g| = 1$.

For the type-II phase $(-1, -1, 2)$, the order of Chern numbers C_2 and C_3 is reversed in contrast to the type-I phase. This results in the changing of the gap Chern number for the higher band gap, which equals $C_g = -2$. For the type-III phase $(2, -1, -1)$, the gap Chern number is altered for the lower band gap, and is given by $C_g = 2$. Here, the gap Chern number greater than one represents the faster evolution propagation of edge states. This has been evidenced in Figs. 4(b), 4(c), where the edge state fluctuates more frequently in the ϕ space. The impulse responses in Figs. 4(f), 4(g) clearly demonstrate that the edge states topologically protected by the large-gap Chern number undergo two complete pumping cycles in one period of evolution. This behavior provides an approach for fast energy transportation of mechanical waves.

For each element of modulated lattices, the constant rotation of rotary-spring mechanisms is required to create the time-varying ground spring and interelement spring. Along with the disturbance of the impulse wave traveling through each element, the external moment of force is

needed for each rotary mechanism to maintain the constant rotation of springs [47,48]. The work done by the moment of force characterizes the energy input into the modulated lattice in the process of adiabatic evolution of edge states. Corresponding to four cases in Figs. 4(d)–4(g), the instantaneous power input P_m for each element in one evolution period is shown in Figs. 5(a)–5(d), where the negative power denotes the energy flowing out of the system. The energy exchange with the surroundings can be clearly observed in space-time paths of the impulse propagation. To quantify the magnitude of input energy, the net work computed by integrating the power input for all elements, $W_{in} = \sum_{\text{all}} \int_0^T P_m dt$, is shown in Figs. 5(e)–5(h), and is compared with the net internal energy E_t , which comprises the kinetic energy of masses and potential energy of springs. The result shows that the input energy is very small in comparison to the magnitude of internal energy of the system. This explains the fact that the adiabatic evolution of edge states does not rely on the external energy input, but is driven by the slow variation of modulated stiffness.

C. Analysis of adiabatic evolution condition

The condition for adiabatic topological evolution can be quantitatively determined using the method based on the adiabatic theorem [52,53]. Here, the method is adopted to analyze the limit speed for adiabaticity in a doubly modulated pumping system. The method is briefly outlined as follows. The kinetic equation describing the free motion of a lattice chain can be generalized into the first-order differential equation, which is expressed by the state vector

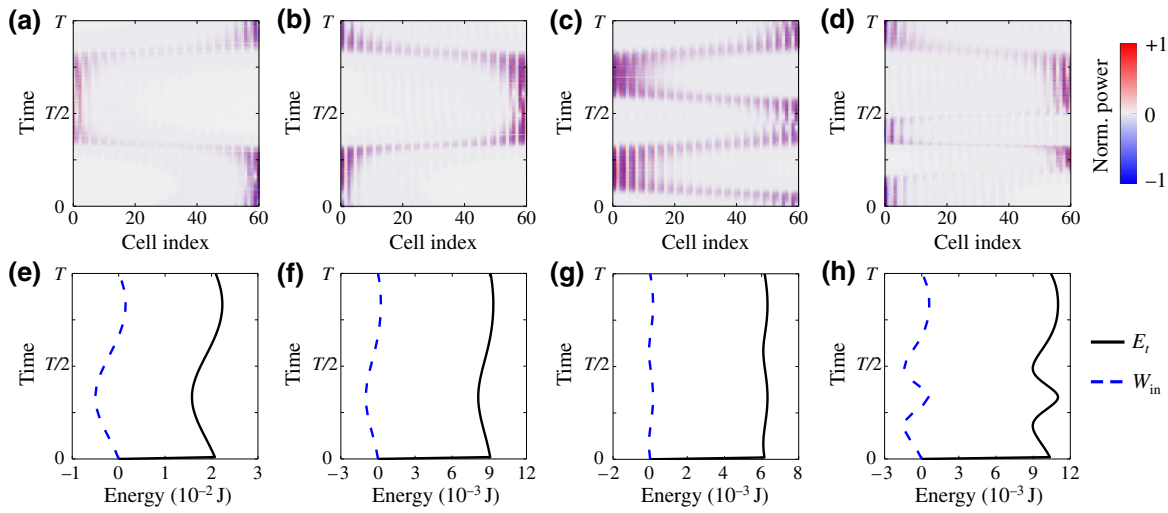


FIG. 5. Energy flow in the process of adiabatic evolution of edge states. (a)–(d) The instantaneous power input for each element in one evolution period, corresponding to four cases in Figs. 4(d)–4(g), and (e)–(h) the net input energy W_{in} for all elements versus the internal energy E_t of the system.

$\psi(t) = [\dot{\mathbf{u}}(t), \mathbf{u}(t)]^T$ as

$$\dot{\psi}(t) = \mathbf{H}(t)\psi(t), \quad (10)$$

$$\mathbf{H}(t) = \begin{bmatrix} \mathbf{0} & -\mathbf{M}^{-1}\mathbf{K}(t) \\ \mathbf{I} & \mathbf{0} \end{bmatrix}, \quad (11)$$

where \mathbf{M} and $\mathbf{K}(t)$ denote the mass and stiffness matrices, and \mathbf{I} is the identity matrix. Introduce the left and right eigenstates of dynamic matrix $\mathbf{H}(t)$, $|L_n(t)\rangle$ and $|R_n(t)\rangle$, which satisfy

$$\mathbf{H}(t)|R_n(t)\rangle = i\omega_n|R_n(t)\rangle, \langle L_n(t)|\mathbf{H}(t) = i\omega_n\langle L_n(t)|, \quad (12)$$

where ω_n is the eigenfrequency. Notice that the left and right eigenstates are normalized satisfying $\langle L_m(t)|R_n(t)\rangle = \delta_{m,n}$ with m, n referring to the band index. The adiabatic

approximation condition is given by [37,54]

$$\alpha = \left| \frac{\langle L_m(t)|\dot{\mathbf{H}}(t)|R_n(t)\rangle}{(\omega_n - \omega_m)^2} \right| \ll 1 \quad (13)$$

for $m \neq n$. The value of α quantitatively describes the interaction of different energy bands. In the adiabatic limit ($\alpha \ll 1$), the system that is initiated from a certain eigenstate will remain in the same state for a sufficiently slow evolution.

The spectral results shown in Figs. 4(a)–4(c) can be adopted to identify the limit speed for adiabatic evolution in a doubly modulated system. The condition in Eq. (13) is applied to two neighboring states, where one state is the topological edge state (e.g., state m), while the other state is chosen as the bulk state (state $n = m \pm 1$) next to the edge mode because other bulk modes give less coupling to the edge state due to greater distance of $|\omega_n - \omega_m|$. Figures 6(a)–6(d) shows the distribution of α against the variation of modulating frequency ω_m and evolution phase

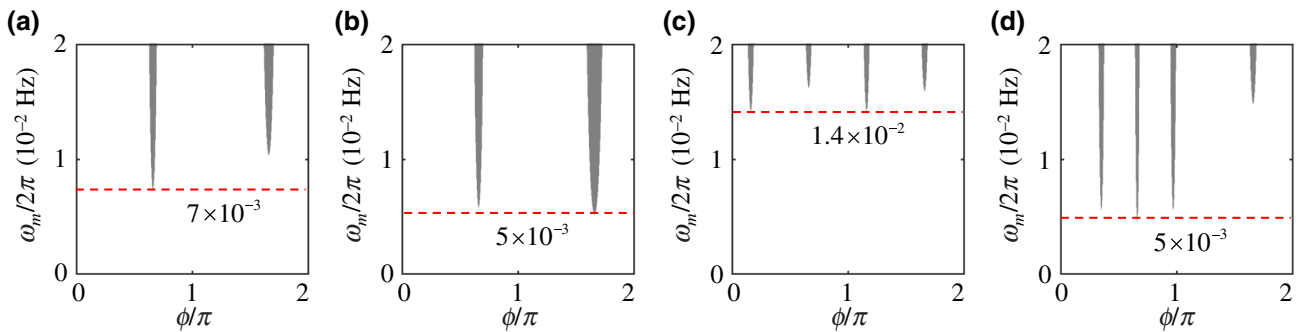


FIG. 6. (a)–(d) Distribution of α against ω_m and ϕ , corresponding to four cases in Figs. 4(d)–4(g), where the region of $\alpha \geq 0.5$ is shaded and recognized as the nonadiabatic region.

ϕ , corresponding to four cases in Figs. 4(d)–4(g). Notice that the region of values $\alpha \geq 0.5$ has been shaded and can be properly recognized as the nonadiabatic region [37]. The limit speeds are then identified and correspond to the modulating frequencies of $\omega_m/2\pi \approx 7 \times 10^{-3}, 5 \times 10^{-3}, 1.4 \times 10^{-2}, 5 \times 10^{-3}$ Hz, respectively. They are all greater than $\omega_m/2\pi = 1 \times 10^{-3}$ Hz adopted in our numerical examples so that the adiabatic approximation is guaranteed. Results also show that the large-gap Chern number does not induce the stronger coupling between edge modes and neighboring bulk states, and the limit speed is not significantly reduced to satisfy the adiabatic approximation. This warrants the fast edge-to-edge energy transportation supported by the large-gap Chern number.

IV. CONCLUSIONS

We investigate the topological pumping in the 1D mass-spring lattice chain where the ground spring and interelement spring are temporally modulated simultaneously. Based on the adiabatic theorem, the time-modulated phase of slow variation of stiffness over time offers a virtual dimension so that the mechanical analogue of the 2D quantum Hall effect is created in 1D lattices. In contrast to the singly modulated scenario, two additional topological phases with the gap Chern number ($|C_g| = 2$) greater than one, termed as type-II $(-1, -1, 2)$ and type-III $(2, -1, -1)$ phases, are found in doubly modulated lattices. The transition of them to type-I phase $(-1, 2, -1)$ is identified by classifying topological phases in the parameter space $(\kappa_1, \kappa_2, \delta\phi_0)$, and the phase transition is found to associate with the closing and reopening of band gaps. The edge states topologically protected by the large-gap Chern number $C_g = \pm 2$ undergo two complete pumping cycles in one period of evolution, leading to the faster edge-to-edge energy propagation as demonstrated numerically. We also analyze the condition for adiabatic evolution in a doubly modulated system, demonstrating that the adiabatic approximation would not be violated for the faster adiabatic pumping of edge states relevant to the large-gap Chern number. We may expect the doubly modulated topological pumping to be used for fast and robust energy transferring of mechanical waves.

ACKNOWLEDGMENTS

This work is supported by the National Natural Science Foundation of China (Grants No. 11872111, No. 11991030, No. 11991033, and No. 11622215) and 111 project (Grant No. B16003).

[1] D. J. Thouless, M. Kohmoto, M. P. Nightingale, and M. den Nijs, Quantized Hall Conductance in a Two-Dimensional Periodic Potential, *Phys. Rev. Lett.* **49**, 405 (1982).

- [2] F. D. M. Haldane, Model for a Quantum Hall Effect Without Landau Levels: Condensed-Matter Realization of the “Parity Anomaly”, *Phys. Rev. Lett.* **61**, 2015 (1988).
- [3] L. Lu, J. D. Joannopoulos, and M. Soljačić, Topological photonics, *Nat. Photonics* **8**, 821 (2014).
- [4] G. Ma, M. Xiao, and C. T. Chan, Topological phases in acoustic and mechanical systems, *Nat. Rev. Phys.* **1**, 281 (2019).
- [5] Z. Wang, Y. Chong, J. D. Joannopoulos, and M. Soljačić, Observation of unidirectional backscattering-immune topological electromagnetic states, *Nature* **461**, 772 (2009).
- [6] Z. Wang, Y. Chong, J. D. Joannopoulos, and M. Soljačić, Reflection-Free One-Way Edge Modes in a Gyromagnetic Photonic Crystal, *Phys. Rev. Lett.* **100**, 013905 (2008).
- [7] A. B. Khanikaev, S. H. Mousavi, W.-K. Tse, M. Kargarian, A. H. MacDonald, and G. Shvets, Photonic topological insulators, *Nat. Mater.* **12**, 233 (2013).
- [8] S. H. Mousavi, A. B. Khanikaev, and Z. Wang, Topologically protected elastic waves in phononic metamaterials, *Nat. Commun.* **6**, 8682 (2015).
- [9] C. He, X. Ni, H. Ge, X.-C. Sun, Y.-B. Chen, M.-H. Lu, X.-P. Liu, and Y.-F. Chen, Acoustic topological insulator and robust one-way sound transport, *Nat. Phys.* **12**, 1124 (2016).
- [10] L. M. Nash, D. Kleckner, A. Read, V. Vitelli, A. M. Turner, and W. T. Irvine, Topological mechanics of gyroscopic metamaterials, *Proc. Natl. Acad. Sci.* **112**, 14495 (2015).
- [11] A. Souslov, B. C. Van Zuiden, D. Bartolo, and V. Vitelli, Topological sound in active-liquid metamaterials, *Nat. Phys.* **13**, 1091 (2017).
- [12] L.-J. Lang, X. Cai, and S. Chen, Edge States and Topological Phases in One-Dimensional Optical Superlattices, *Phys. Rev. Lett.* **108**, 220401 (2012).
- [13] Y. E. Kraus and O. Zilberberg, Quasiperiodicity and topology transcend dimensions, *Nat. Phys.* **12**, 624 (2016).
- [14] Y. E. Kraus, Z. Ringel, and O. Zilberberg, Four-Dimensional Quantum Hall Effect in a Two-Dimensional Quasicrystal, *Phys. Rev. Lett.* **111**, 226401 (2013).
- [15] Z.-G. Chen, W. Zhu, Y. Tan, L. Wang, and G. Ma, Acoustic Realization of a Four-Dimensional Higher-Order Chern Insulator and Boundary-Modes Engineering, *Phys. Rev. X* **11**, 011016 (2021).
- [16] I. Petrides and O. Zilberberg, Higher-order topological insulators, topological pumps and the quantum hall effect in high dimensions, *Phys. Rev. Res.* **2**, 022049 (2020).
- [17] H. Chen, H. Zhang, Q. Wu, Y. Huang, H. Nguyen, E. Prodan, X. Zhou, and G. Huang, Creating synthetic spaces for higher-order topological sound transport, *Nat. Commun.* **12**, 5028 (2021).
- [18] D. Thouless, Quantization of particle transport, *Phys. Rev. B* **27**, 6083 (1983).
- [19] D. R. Hofstadter, Energy levels and wave functions of bloch electrons in rational and irrational magnetic fields, *Phys. Rev. B* **14**, 2239 (1976).
- [20] S. Aubry and G. André, Analyticity breaking and anderson localization in incommensurate lattices, *Ann. Israel Phys. Soc.* **3**, 18 (1980).
- [21] M. Lohse, C. Schweizer, O. Zilberberg, M. Aidelsburger, and I. Bloch, A thouless quantum pump with ultracold bosonic atoms in an optical superlattice, *Nat. Phys.* **12**, 350 (2016).

- [22] S. Nakajima, T. Tomita, S. Taie, T. Ichinose, H. Ozawa, L. Wang, M. Troyer, and Y. Takahashi, Topological thouless pumping of ultracold fermions, *Nat. Phys.* **12**, 296 (2016).
- [23] M. Lohse, C. Schweizer, H. M. Price, O. Zilberberg, and I. Bloch, Exploring 4D quantum Hall physics with a 2D topological charge pump, *Nature* **553**, 55 (2018).
- [24] O. Zilberberg, S. Huang, J. Guglielmon, M. Wang, K. P. Chen, Y. E. Kraus, and M. C. Rechtsman, Photonic topological boundary pumping as a probe of 4D quantum Hall physics, *Nature* **553**, 59 (2018).
- [25] Y. E. Kraus, Y. Lahini, Z. Ringel, M. Verbin, and O. Zilberberg, Topological States and Adiabatic Pumping in Quasicrystals, *Phys. Rev. Lett.* **109**, 106402 (2012).
- [26] Y. Ke, X. Qin, F. Mei, H. Zhong, Y. S. Kivshar, and C. Lee, Topological phase transitions and thouless pumping of light in photonic waveguide arrays, *Laser Photonics Rev.* **10**, 995 (2016).
- [27] X. Xu, Q. Wu, H. Chen, H. Nassar, Y. Chen, A. Norris, M. R. Haberman, and G. Huang, Physical Observation of a Robust Acoustic Pumping in Waveguides with Dynamic Boundary, *Phys. Rev. Lett.* **125**, 253901 (2020).
- [28] W. Cheng, E. Prodan, and C. Prodan, Experimental Demonstration of Dynamic Topological Pumping across Incommensurate Bilayered Acoustic Metamaterials, *Phys. Rev. Lett.* **125**, 224301 (2020).
- [29] X. Ni, K. Chen, M. Weiner, D. J. Apigo, C. Prodan, A. Alu, E. Prodan, and A. B. Khanikaev, Observation of hofstadter butterfly and topological edge states in reconfigurable quasi-periodic acoustic crystals, *Commun. Phys.* **2**, 55 (2019).
- [30] Y. Long and J. Ren, Floquet topological acoustic resonators and acoustic thouless pumping, *J. Acoust. Soc. Am.* **146**, 742 (2019).
- [31] Z.-G. Chen, W. Tang, R.-Y. Zhang, Z. Chen, and G. Ma, Landau-Zener Transition in the Dynamic Transfer of Acoustic Topological States, *Phys. Rev. Lett.* **126**, 054301 (2021).
- [32] Z. Chen, Z. Chen, Z. Li, B. Liang, G. Ma, Y. Lu, and J. Cheng, Topological pumping in acoustic waveguide arrays with hopping modulation, *New J. Phys.* **24**, 013004 (2021).
- [33] Y.-X. Shen, Y.-G. Peng, D.-G. Zhao, X.-C. Chen, J. Zhu, and X.-F. Zhu, One-Way Localized Adiabatic Passage in an Acoustic System, *Phys. Rev. Lett.* **122**, 094501 (2019).
- [34] Y.-X. Shen, L.-S. Zeng, Z.-G. Geng, D.-G. Zhao, Y.-G. Peng, and X.-F. Zhu, Acoustic Adiabatic Propagation Based on Topological Pumping in a Coupled Multicavity Chain Lattice, *Phys. Rev. Appl.* **14**, 014043 (2020).
- [35] Y.-X. Shen, L.-S. Zeng, Z.-G. Geng, D.-G. Zhao, Y.-G. Peng, J. Zhu, and X.-F. Zhu, Acoustic topological adiabatic passage via a level crossing, *SCIENCE CHINA Physics, Mechanics Astronomy* **64**, 244302 (2021).
- [36] L.-S. Zeng, Y.-X. Shen, Y.-G. Peng, D.-G. Zhao, and X.-F. Zhu, Selective Topological Pumping for Robust, Efficient, and Asymmetric Sound Energy Transfer in a Dynamically Coupled Cavity Chain, *Phys. Rev. Appl.* **15**, 064018 (2021).
- [37] Y. Xia, E. Riva, M. I. Rosa, G. Cazzulani, A. Erturk, F. Braghin, and M. Ruzzene, Experimental Observation of Temporal Pumping in Electromechanical Waveguides, *Phys. Rev. Lett.* **126**, 095501 (2021).
- [38] M. I. Rosa, Y. Guo, and M. Ruzzene, Exploring topology of 1d quasiperiodic metastructures through modulated lego resonators, *Appl. Phys. Lett.* **118**, 131901 (2021).
- [39] Y. Xia, A. Erturk, and M. Ruzzene, Topological Edge States in Quasiperiodic Locally Resonant Metastructures, *Phys. Rev. Appl.* **13**, 014023 (2020).
- [40] E. Riva, M. I. Rosa, and M. Ruzzene, Edge states and topological pumping in stiffness-modulated elastic plates, *Phys. Rev. B* **101**, 094307 (2020).
- [41] I. H. Grinberg, M. Lin, C. Harris, W. A. Benalcazar, C. W. Peterson, T. L. Hughes, and G. Bahl, Robust temporal pumping in a magneto-mechanical topological insulator, *Nat. Commun.* **11**, 974 (2020).
- [42] M. I. Rosa, R. K. Pal, J. R. Arruda, and M. Ruzzene, Edge States and Topological Pumping in Spatially Modulated Elastic Lattices, *Phys. Rev. Lett.* **123**, 034301 (2019).
- [43] M. Yahyavi, B. Hetényi, and B. Tanatar, Generalized Aubry-andré-harper model with modulated hopping and p-wave pairing, *Phys. Rev. B* **100**, 064202 (2019).
- [44] H. Nassar, H. Chen, A. Norris, and G. Huang, Quantization of band tilting in modulated phononic crystals, *Phys. Rev. B* **97**, 014305 (2018).
- [45] H. Chen, L. Yao, H. Nassar, and G. Huang, Mechanical Quantum Hall Effect in Time-Modulated Elastic Materials, *Phys. Rev. Appl.* **11**, 044029 (2019).
- [46] R. K. Pal, M. I. Rosa, and M. Ruzzene, Topological bands and localized vibration modes in quasiperiodic beams, *New J. Phys.* **21**, 093017 (2019).
- [47] J. Huang and X. Zhou, A time-varying mass metamaterial for non-reciprocal wave propagation, *Int. J. Solids Struct.* **164**, 25 (2019).
- [48] J. Huang and X. Zhou, Non-reciprocal metamaterials with simultaneously time-varying stiffness and mass, *J. Appl. Mech.* **87**, 071003 (2020).
- [49] T. Fukui, Y. Hatsugai, and H. Suzuki, Chern numbers in discretized brillouin zone: Efficient method of computing (spin) hall conductances, *J. Phys. Soc. Jpn.* **74**, 1674 (2005).
- [50] Y. Hatsugai and T. Fukui, Bulk-edge correspondence in topological pumping, *Phys. Rev. B* **94**, 041102 (2016).
- [51] B. A. Bernevig, *Topological Insulators and Topological Superconductors* (Princeton University Press, Princeton, USA, 2013).
- [52] X. Yi, D. Tong, L. Kwek, and C. Oh, Adiabatic approximation in open systems: An alternative approach, *J. Phys. B: At. Mol. Opt. Phys.* **40**, 281 (2007).
- [53] M. H. Amin, Consistency of the Adiabatic Theorem, *Phys. Rev. Lett.* **102**, 220401 (2009).
- [54] E. Riva, G. Castaldini, and F. Braghin, Adiabatic edge-to-edge transformations in time-modulated elastic lattices and non-hermitian shortcuts, *New J. Phys.* **23**, 093008 (2021).